Celsr3 is required in motor neurons to steer their axons in the hindlimb

Guoliang Chai[1], Libing Zhou[2], Mario Manto[3], Françoise Helmbacher[4], Frédéric Clotman[5], André M Goffinet[1,6] & Fadel Tissir[1]

The cadherin Celsr3 regulates the directional growth and targeting of axons in the CNS, but whether it acts in collaboration with or in parallel to other guidance cues is unknown. Furthermore, the function of Celsr3 in the peripheral nervous system is still largely unexplored. Here we show that Celsr3 mediates pathfinding of motor axons innervating the hindlimb. In mice, Celsr3-deficient axons of the peroneal nerve segregate from those of the tibial nerve but fail to extend dorsally, and they stall near the branch point. Mutant axons respond to repulsive ephrinA-EphA forward signaling and glial cell–derived neurotrophic factor (GDNF). However, they are insensitive to attractive EphA-ephrinA reverse signaling. In transfected cells, Celsr3 immunoprecipitates with ephrinA2, ephrinA5, Ret, GDNF family receptor α1 (GFRα1) and Frizzled3 (Fzd3). The function of Celsr3 is Fzd3 dependent but Vangl2 independent. Our results provide evidence that the Celsr3-Fzd3 pathway interacts with EphA-ephrinA reverse signaling to guide motor axons in the hindlimb.

A crucial event during the development of the nervous system is the establishment of complex and precise connections between neurons and their targets. This is achieved by a repertoire of repulsive and attractive cues that instruct axons when and where to leave, progress forward or turn, and where to halt[1]. An example is the guidance of motor axons projecting into the hindlimb. Motor neurons that innervate the hindlimb are located in the lateral motor column (LMC) of the lumbar spinal cord and initially send their axons through the sciatic nerve. As they reach the base of the limb, axons of motor neurons located in the lateral division of the LMC (LMC_L) turn dorsally and form the peroneal nerve, whereas those from the medial division (LMC_M) select a ventral trajectory and form the tibial nerve[2–5]. Loss- and gain-of-function studies in mouse and chicken have shown that ephrinA-EphA (hereafter "EphA") forward signaling is important for the segregation of motor axons with dorsal or ventral fates. LMC_L EphA4-rich growth cones are repelled by ephrinA in the ventral mesenchyme. In *Epha4* mutant mice, LMC_L axons fail to grow dorsally and instead run ventrally in the tibial nerve[6]. Conversely, ectopic expression of EphA4 in LMC_M neurons reroutes their axons into the dorsal limb[7,8]. A further complexity is that EphA and ephrinA are coexpressed in both LMC_L neurons and limb mesenchyme, and their interactions *in trans* generate bidirectional signals[9]. In addition to the repulsive EphA forward signaling, EphAs expressed in dorsal mesenchymal cells bind ephrinAs in motor axons and generate an "ephrinA" reverse signaling that mediates dorsal attraction of LMC_L axons in a Ret-dependent manner[10–12]. Furthermore, analysis of *Gdnf*, *Gfra1* and *Ret* mutant mice showed that GDNF, secreted dorsally to the branching point, binds to GFRα1 and Ret on the growth cones of LMC_L axons and that this reinforces their dorsal fate[12,13].

Celsr3 is a seven-pass cadherin with known functions in axon pathfinding. Celsr3-deficient mice exhibit marked defects in several cortico-cortical and cortico-subcortical connections, such as the anterior commissure, internal capsule and corticospinal tract[14,15]. Celsr3 is also implicated in guidance of monoaminergic axons along the anterior-posterior axis[16] and in the anterior turning of commissural axons in the spinal cord[17,18]. Celsr3 deficiency does not alter axonal growth, but affects axon guidance in both cell-autonomous and non-cell-autonomous manners, thus causing axon stalling at intermediate targets or rerouting[14,15]. Notably, *Celsr3*$^{-/-}$ phenotypes were also observed in mice bearing mutations in the planar cell polarity (PCP) gene *Fzd3* (refs. 19–21), and errors in axon guidance of monoaminergic and commissural neurons were reported in mice with the looptail mutation in *Vangl2*, another PCP gene[16,22].

Despite its importance in axon guidance in the CNS, the role of Celsr3 in the peripheral nervous system (PNS) has not been investigated. Moreover, the mechanisms of action of Celsr3 are not completely understood. In this work, we show that *Celsr3* controls the navigation of motor axons innervating the dorsal hindlimb. Inactivation of *Celsr3* severely perturbed peroneal nerve development. While mutant axons were still able to respond to EphA forward signaling and GDNF, they lost responsiveness to attractive ephrinA reverse signaling. Physical interactions between Celsr3/Fzd3, ephrinAs, Ret and GFRα1 suggest that they belong to the same guidance toolbox.

[1]Developmental Neurobiology, Institute of Neuroscience, Université catholique de Louvain, Brussels, Belgium. [2]Guangdong-Hongkong-Macau Institute of CNS Regeneration, Jinan University, Guangzhou, China. [3]Unité d'Etude du Mouvement (UEM), Neurologie, Erasme, Université Libre de Bruxelles, Brussels, Belgium. [4]Centre National de la Recherche Scientifique, Institut de Biologie du Développement de Marseille Luminy, Aix-Marseille Université, Marseille, France. [5]Laboratory of Neural Differentiation, Institute of Neuroscience, Université catholique de Louvain, Brussels, Belgium. [6]Developmental Neurobiology, WELBIO, Brussels, Belgium. Correspondence should be addressed to F.T. (fadel.tissir@uclouvain.be).

Received 14 May; accepted 15 July; published online 10 August 2014; doi:10.1038/nn.3784

RESULTS

Celsr3 mutant mice have a clubfoot-like phenotype

Celsr3 constitutive knockout (*Celsr3*$^{-/-}$) mice exhibited a hindlimb phenotype reminiscent of congenital talipes equinovarus, also known as clubfoot, in humans. The ankle and the heel were twisted inwardly and the sole of the foot was inverted (**Fig. 1a**). To understand the role of Celsr3 in this context, we first studied its expression in the developing limb and the lumbar spinal cord using *in situ* hybridization. The *Celsr3* transcript was restricted to postmitotic neurons in the spinal cord and dorsal root ganglia, with no signal in the limb bud, suggesting that the contribution of Celsr3 to the phenotype is related to its expression in neurons (**Fig. 1b**,**c**).

The effect of Celsr3 ablation could be direct, affecting motor neurons, or indirect, secondary to defective wiring within the spinal cord, with impact on motor neurons' function. To discriminate these possibilities, we generated conditional mutants by crossing *Celsr3*$^{fl/-}$ mice, with a *loxP*-flanked (floxed; *fl*) allele, with mice expressing the Cre recombinase under the control of the following gene promoters: *Isl1* (motor neurons and neural crest derivatives; **Supplementary Fig. 1a**–**f**)[23], *Olig2* (motor neurons and oligodendrocyte lineage; **Supplementary Fig. 1g**)[24] or *Wnt1* (sensory neurons; **Supplementary Fig. 1e**)[25,26]. *Celsr3*$^{fl/-}$;*Isl1::Cre* and *Celsr3*$^{fl/-}$;*Olig2::Cre* adult mice exhibited defective locomotor behavior, with unilateral or bilateral paralysis of the hindlimb (**Fig. 1d**, **Supplementary Movie 1** and **Supplementary Movie 2**). In sharp contrast, *Celsr3*$^{fl/-}$;*Wnt1::Cre* mice never displayed hindlimb abnormalities (**Supplementary Fig. 1i**; $n = 16$ embryos and 20 adults). In *Celsr3*$^{fl/-}$;*Isl1::Cre* adult mice, the thickness of the sciatic nerve and the number of motor axons were reduced by 44% (**Fig. 1e**,**f**; $n = 5$; $P = 0.0079$, Mann-Whitney test). Muscles in the anterior compartment, particularly the tibialis anterior, were severely atrophied (**Fig. 1g**,**h**). These muscles control ankle movements, and their dysfunction is a recognized cause of clubfoot. We analyzed motor innervation and neuromuscular junctions in newborn animals and found that dorsal muscles were not innervated (**Fig. 1i**,**j**). α-bungarotoxin staining showed a prominent increase in the number of postsynaptic receptors, a typical feature of denervated muscles[27]. We recorded the compound muscle action potentials (CMAPs) from tibialis anterior muscles in response to direct supramaximal stimuli applied to the sciatic nerve[28]. In contrast to the wild type CMAP responses, characterized by a typical biphasic wave, the CMAPs were polyphasic (more than four phases) in the paralyzed mutants, with lower amplitudes and prolonged latencies, indicating a collateral reinnervation following defective developmental innervation (**Fig. 1k**,**l**).

Abnormal peroneal nerve in *Celsr3*$^{-/-}$ mutant mice

Lack of innervation of the tibialis anterior muscle in *Celsr3* mutant mice could have two origins: either motor axons never reach the muscle during embryonic development, or they initially do but retract later owing to death of motor neurons. To investigate these possibilities, we examined the development of the sciatic nerve using neurofilament staining and *Hb9::GFP* (also known as *Hlxb9::GFP*) labeling at embryonic (E) days E11.5 and E12.5. In the wild type, the sciatic nerve first divides into ventral and dorsal trunks. The ventral trunk gives rise to the tibial nerve, and the dorsal to the common peroneal nerve, which divides further into superficial and deep peroneal nerves (**Fig. 2a**–**c**). The superficial peroneal nerve innervates the lateral and dorsal part of the hindlimb and the dorsum of the foot, whereas the deep peroneal nerve innervates muscles of the anterior compartment, such as the tibialis anterior and extensor digitorum longus. Whereas the tibial nerve was normal in *Celsr3*$^{-/-}$ embryos, the peroneal nerve was thinner in 67% of these embryos than in wild type littermates (**Fig. 2d**–**f**,**j**) and severely truncated in the remaining 33% (**Fig. 2g**–**i**,**j**). Similar defects were observed in *Celsr3*$^{fl/-}$;*Isl1::Cre* and *Celsr3*$^{fl/-}$;*Olig2::Cre*, but not in *Celsr3*$^{fl/-}$;*Wnt1::Cre* embryos (**Fig. 2j** and **Supplementary Fig. 1h**–**k**).

In the CNS, *Celsr2* and *Celsr3* have overlapping expression patterns and redundant functions[29,30]. To assess the function of *Celsr2* in peroneal nerve development, we studied its expression by *in situ* hybridization. *Celsr2* was ubiquitously expressed in the lumbar spinal cord and dorsal root ganglia (**Fig. 2k**,**l**). In *Celsr2*$^{-/-}$ embryos, the size and length of the

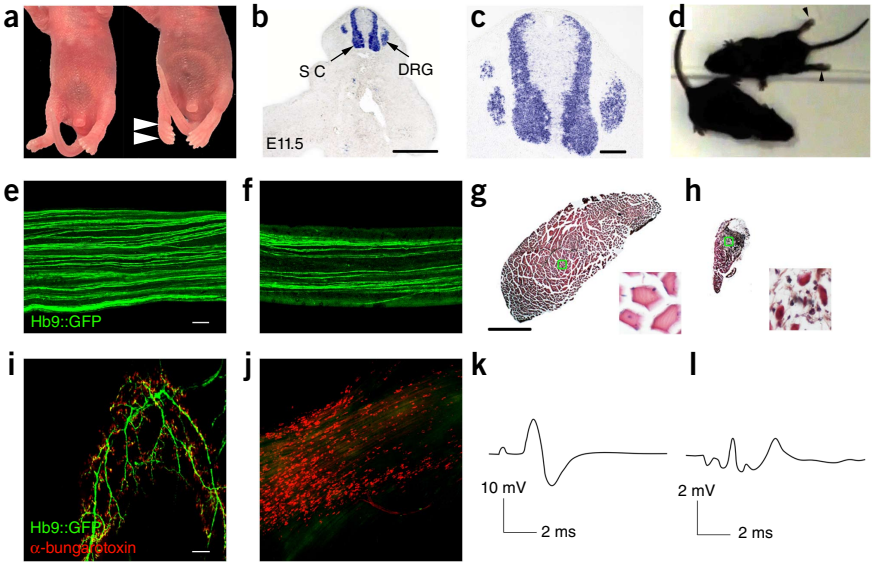

Figure 1 Defective hindlimb innervation in *Celsr3* mutant mice. (**a**) Limb morphology in wild type (left) and *Celsr3*$^{-/-}$ (right) newborns. Note the distorted ankle and clubfoot in the mutant (arrowheads). (**b**) Transverse section of an E11.5 embryo at lumbar level of the spinal cord hybridized with a *Celsr3* digoxigenin-labeled probe. *Celsr3* is not expressed in the limb mesenchyme. The experiment was performed twice. (**c**) *In situ* hybridization of *Celsr3* on transverse sections of lumbar spinal cord at E11.5. *Celsr3* mRNA is expressed in all postmitotic neurons, including neurons in medial and lateral motor columns. (**d**) Picture extracted from **Supplementary Movie 1**. A postnatal day (P) 21 *Celsr3*$^{fl/-}$;*Isl1::Cre* mouse (top) exhibits stiff hindlimbs (arrowheads) compared to wild type (bottom). (**e**,**f**) Whole mount of P21 sciatic nerves labeled with Hb9::GFP, from wild type (**e**) and *Celsr3*$^{fl/-}$;*Isl1::Cre* (**f**) mice. (**g**,**h**) Hematoxylin and eosin–stained sections of tibialis anterior (TA) muscles of P21 wild type (**g**) and paralyzed *Celsr3*$^{fl/-}$;*Isl1::Cre* (**h**) mice. Insets are enlargement of the outlined regions (green). The staining was repeated 3 times ($n = 3$ mice per genotype). (**i**,**j**) Neuromuscular junctions in the TA muscles of wild type (**i**) and paralyzed *Celsr3*$^{fl/-}$;*Isl1::Cre* (**j**) mice at P0. Motor axons (green) are labeled with *Hb9::GFP*, and postsynaptic buttons (red) are detected using α-bungarotoxin immunofluorescence. The staining was repeated at least 4 times ($n = 4$ mice per genotype). (**k**,**l**) Recordings of the compound muscle action potentials from the TA muscles of adult wild type (**k**) and paralyzed *Celsr3*$^{fl/-}$;*Isl1::Cre* (**l**) mice. DRG, dorsal root ganglia; SC, spinal cord. Scale bars: 500 μm (**b**), 100 μm (**c**,**e**,**i**), 1 mm (**g**). Scale bars in **e**, **g** and **i** apply to **f**, **h** and **j**, respectively.

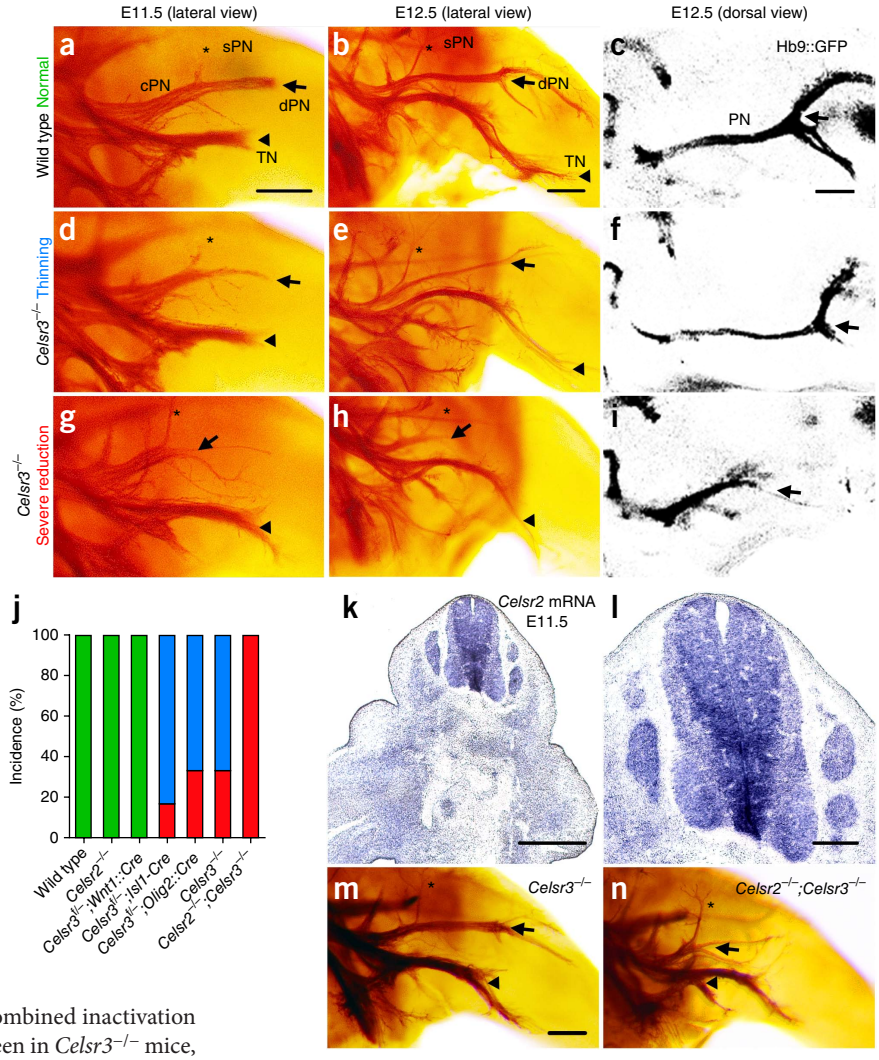

Figure 2 Reduction of dorsal limb innervation in *Celsr3* mutant mice. (**a**–**i**) Axon projections in wild type (**a**–**c**) and *Celsr3*$^{-/-}$ (**d**–**i**) embryos. Lateral views of sciatic nerve projections revealed by anti–neurofilament 160 staining in wild type (**a**,**b**) and *Celsr3*$^{-/-}$ embryos (**d**,**e**,**g**,**h**) at E11.5 and E12.5. Distal is to the right, dorsal is up. In wild type (**a**,**b**), the sciatic nerve divides into ventral tibial nerve (TN, arrowhead) and the dorsal common peroneal nerve (cPN), which further divides into superficial (sPN, asterisk) and deep (dPN, arrow) peroneal nerves. In *Celsr3*$^{-/-}$ embryos, the peroneal nerve is either thinner (**d**,**e**) or severely reduced with loss of the most distal branches (**g**,**h**). (**c**,**f**,**i**) Dorsal views of the peroneal nerve labeled by *Hb9::GFP* at E12.5. The peroneal nerve is reduced in *Celsr3*$^{-/-}$ (**f**,**i**) relative to wild type (**c**). Distal is right. (**j**) Incidence of phenotypic severity in *Celsr2* and *Celsr3* mutants. Green, normal; blue, thinning; red, severe reduction. Wild type, $n = 32$; *Celsr2*$^{-/-}$, $n = 16$; *Celsr3*$^{fl/-}$;*Wnt1::Cre*, $n = 16$; *Celsr3*$^{fl/-}$;*Isl1::Cre*, $n = 30$; *Celsr3*$^{fl/-}$;*Olig2::Cre*, $n = 20$; *Celsr3*$^{-/-}$, $n = 52$; *Celsr2*$^{-/-}$;*Celsr3*$^{-/-}$, $n = 14$. (**k**,**l**) Transverse sections from E11.5 embryos at the level of the lumbar spinal cord and hindlimbs, hybridized with a *Celsr2* probe. The experiment was performed twice. (**m**,**n**) Whole-mount neurofilament staining of hindlimbs from *Celsr2*$^{-/-}$ and *Celsr2*$^{-/-}$;*Celsr3*$^{-/-}$ embryos at E12.5. Scale bars: 200 µm (**a**–**c**,**m**); 500 µm (**k**); 100 µm (**l**). Scale bar in **a** applies to **d** and **g**, bar in **b** to **e** and **h**, bar in **c** to **f** and **i**, and bar in **m** to **n**.

peroneal nerve were undistinguishable from those of controls, and no hindlimb deformity was seen in *Celsr2*$^{-/-}$ adult mice. However, the combined inactivation of *Celsr2* and *Celsr3* exacerbated the phenotype seen in *Celsr3*$^{-/-}$ mice, increasing the percentage of the truncated form to 100% (**Fig. 2j**,**m**,**n**).

Stalling of mutant axons in the dorsal limb

In *Celsr3* mutants, very few, if any, LMC_L axons reach their targets. One possibility could be that LMC_L neurons are not correctly specified. To test this hypothesis, we used Isl1 and Foxp1 immunostaining in lumbar spinal cord sections. Foxp1 labels neurons of LMC_M and LMC_L, Isl1 those of the medial motor column and LMC_M. We compared the total number of LMC neurons, as well as the ratio of LMC_L to LMC_M, and did not find any difference between *Celsr3* mutants and controls at E11.5 (**Supplementary Fig. 2a**–**c**) or E12.5 (**Fig. 3a**,**b**; mean LMC_L/LMC_M ratio 0.9554 in wild type and 0.9474 in *Celsr3*$^{-/-}$; mean number of LMC neurons 4,673 for wild type and 4,771 neurons for *Celsr3*$^{-/-}$; 4 embryos for each genotype; $P = 0.8571$, Mann-Whitney test), demonstrating that neurons of the LMC_L were correctly specified. To test whether LMC_L axons were rerouted ventrally, as in *Epha4*, *Gdnf*, *Ret* or *Gfra1* mutants, we injected rhodamine dextran into the tibial nerve. This resulted in back-labeling of LMC_M but not LMC_L cell bodies, showing that LMC_L axons did not project in the tibial nerve in *Celsr3* mutants (**Fig. 3c**–**e**, percentage of LMC_L neurons labeled 3.433% in wild type and 3.597% in *Celsr3*$^{-/-}$; 3 wild type, 6 *Celsr3*$^{-/-}$; $P = 0.7000$, Mann-Whitney test). We measured the width of the tibial nerve and found that it was similar in wild type and mutant embryos (mean widths 64.3 and 63.6 µm in wild type and *Celsr3*$^{-/-}$, respectively). We measured the width of the common peroneal nerve and found that it was similar in the two genotypes, suggesting that axons of the LMC_L reach the proximal part of the common peroneal nerve in *Celsr3*$^{-/-}$ embryos (mean thickness 61.1 µm in the wild type and 57.8 µm in *Celsr3*$^{-/-}$; **Fig. 3f**–**h**). By contrast, the width of the deep peroneal nerve was dramatically reduced in *Celsr3*$^{-/-}$ embryos as compared to control littermates (mean thickness 48.8 µm in the wild type and 29.7 µm in *Celsr3*$^{-/-}$; **Fig. 3f**–**h**).

We crossed *Celsr3* mutants to *Lhx1*^{tlz} mice (also known as *Lim1*^{tlz}; ref. 31) to specifically label LMC_L axons and confirmed that those axons do not project to the tibial nerve, but stall at the location from which the first branch of the peroneal nerve emerges (**Fig. 3i**,**j**). Finally, we stained lumbar spinal cord sections with cleaved caspase 3 antibodies and did not detect any difference between mutants and controls at E11.5 or E12.5 (**Supplementary Fig. 2a**,**b**). At E13.5, the number of apoptotic cells was slightly but significantly higher in *Celsr3*$^{-/-}$ mice than in controls (**Fig. 3k**,**l** and **Supplementary Fig. 2**; 2.6-fold increase in mutant, 4 embryos for each genotype, $P = 0.0054$, Mann-Whitney test). Consistent with this finding, the total number of LMC neurons was lower in mutants than in wild type embryos. Cell death occurred mostly in LMC_L, which led to a reduced LMC_L/LMC_M ratio (**Supplementary Fig. 2d**). In *Celsr2*$^{-/-}$;*Celsr3*$^{-/-}$ double mutants, the number of apoptotic cells was higher than in wild type and *Celsr3*$^{-/-}$ mice (**Supplementary Fig. 2e**–**g**). Taken together, these results show that LMC_L motor axons reach the dorsoventral

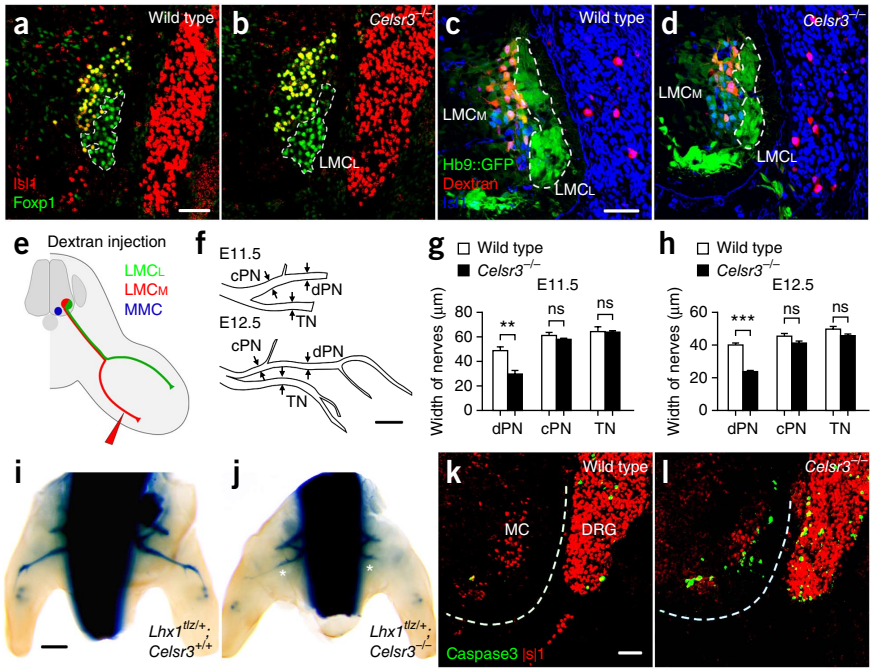

Figure 3 Celsr3-deficient LMC_L axons fail to extend in the dorsal limb. (**a**,**b**) Transverse sections of lumbar spinal cord at E12.5 from wild type (**a**) and *Celsr3* mutant embryos (**b**), stained with Foxp1 (green) and Isl1 (red) antibodies. LMC_L neurons are Foxp1-positive and Isl1-negative, whereas LMC_M neurons are Foxp1- and Isl1-positive. The staining was repeated 4 times ($n = 4$ embryos per genotype). (**c**,**d**) Injection of rhodamine dextran (red) into the ventral tibial nerve labels selectively LMC_M neurons (*Hb9::GFP*, green; Isl1-positive, blue) in wild type (**c**) and *Celsr3*$^{-/-}$ (**d**) E13.5 embryos. The staining was repeated at least 6 times ($n = 6$ embryos for *Celsr3*$^{-/-}$ and 3 for wild type). (**e**) Schematic view of the developing limb showing the site of injection of rhodamine dextran near the extremity of the ventral nerve. (**f**) Schematic drawing of the sciatic nerve at E11.5 and E12.5. Three positions were selected to measure the width: deep peroneal nerve (dPN), common peroneal nerve (cPN) and tibial nerve (TN). (**g**,**h**) Quantification of the nerve width at E11.5 (**g**) and E12.5 (**h**). cPN and TN were not affected in *Celsr3*$^{-/-}$ embryos (E11.5, 8 wild type and 16 mutants, $P = 0.1921$ for cPN and 0.8111 for TN; E12.5, 12 wild type and 10 mutants, $P = 0.0685$ for cPN, and 0.0608 for TN). The deep peroneal nerve was significantly reduced in *Celsr3*$^{-/-}$ embryos (E11.5, 8 wild type and 16 mutants, $P = 0.0019$; E12.5, 12 wild type and 10 mutants, $P < 0.0001$, unpaired *t*-test; error bars are mean ± s.e.m.). (**i**,**j**) Whole mount β-galactosidase staining of hindlimbs from *Lhx1*$^{tlz/+}$*;Celsr3*$^{+/+}$ (**i**) and *Lhx1*$^{tlz/+}$*;Celsr3*$^{-/-}$ (**j**) E12.5 embryos. Note the severe reduction of the deep peroneal nerve on the left and its absence on the right side of the mutant embryo (asterisks; the staining was repeated at least 8 times). (**k**,**l**) Cleaved caspase 3 (green) and Isl1 (red) immunostaining on lumbar spinal cord transverse sections from E13.5 wild type (**k**) and *Celsr3*$^{-/-}$ (**l**) embryos. The staining was repeated at least 4 times ($n = 4$ embryos per genotype). Scale bars: 50 μm (**a**,**c**,**k**); 200 μm (**f**,**i**). Scale bars in **a**, **c**, **i** and **k** apply to **b**, **d**, **j** and **l**, respectively.

bifurcation of the sciatic nerve and segregate from axons of the tibial nerve, but do not form the deep peroneal nerve. Therefore, they cannot innervate target muscles, and they most likely retract and degenerate because of lack of target-derived growth factors.

Mutant axons are insensitive to ephrinA reverse signaling

When LMC_L axons reach the limb bud, they encounter a variety of cues that guide them to their targets in the dorsal limb. EphA forward signaling (EphA4 in the growth cone and ephrinAs in the ventral mesenchyme) prevents them from invading the ventral limb, whereas ephrinA reverse signaling (ephrinA2 and ephrinA5 in growth cones; EphA3, EphA4 and EphA7 in the dorsal mesenchyme) and GDNF attract them to the dorsal limb. We analyzed the expression of several axon guidance molecules in the spinal cord and hindlimb and did not find any difference between wild type and mutant embryos (**Supplementary Fig. 3a–r**). We studied the behavior of Celsr3-deficient LMC axons using *in vitro* assays. We isolated LMC from *Hb9::GFP* transgenic embryos at E12.5 and cultured dissociated neurons or explants on laminin-coated coverslips. We did not find any difference between wild type and *Celsr3*$^{-/-}$ mutants in terms of neuronal survival or neurite outgrowth, suggesting that Celsr3 is not essential to these processes (**Supplementary Fig. 4a–g**). We then plated explants on coverslips printed with alternating stripes of IgG-Fc/IgG-Fc (human IgG_1 Fc fragment) or IgG-Fc/ephrinA5-Fc (human ephrinA5 fused with human IgG_1 Fc fragment). GFP-positive LMC axons from both wild type and *Celsr3*$^{-/-}$ embryos grew preferentially on IgG-Fc stripes and avoided the ephrinA5-Fc stripes (**Fig. 4a–d**).

In *Gdnf*, *Ret* or *Gfra1* mutant mice, innervation of the cutaneus maximus and latissimus dorsi back muscles by brachial motor axons is completely lost, showing that the interaction between GDNF, secreted by mesenchymal cells, and Ret and GFRα1 in the growth cone is essential to this process[12,32]. To probe whether Celsr3, which is expressed in all motor neurons, is implicated in the response of motor axons to GDNF, we examined brachial motor axon projections in *Celsr3*$^{-/-}$*;Hb9::GFP* embryos. At E12.5, these projections were similar to those in wild type littermates (**Supplementary Fig. 5a,b**). We also analyzed the response of lumbar motor axons to a point source of GDNF. Compared to BSA, GDNF triggered a strong axonal growth in wild type and Celsr3-deficient explants alike, suggesting that Celsr3 is dispensable in motor axons for the response to GDNF (**Fig. 4e–h**). Taken together, these data show that loss of Celsr3 function does not alter the responsiveness of LMC axons to the repulsive effect of EphA forward signaling or to GDNF.

To assess the response of Celsr3-deficient LMC axons to attractive ephrinA reverse signaling, we cultured LMC explants on coverslips coated with either clustered IgG-Fc or EphA7-Fc, together with a low concentration of laminin (5 μg/ml)[4,10]. With both wild type and *Celsr3*$^{-/-}$ explants, axonal growth was limited on IgG-Fc substrate (**Fig. 4i,k**). Remarkably, EphA7 enhanced axonal outgrowth only in wild type and not in *Celsr3*$^{-/-}$ explants (**Fig. 4i–m**; fold induction of axon outgrowth by EphA7-Fc versus IgG-Fc: 2.73 for wild type and 1.36 for *Celsr3*$^{-/-}$; $n = 73$ explants on IgG and 70 on EphA7 from 6 wild type embryos, $n = 42$ explants on IgG and 39 on EphA7 from 3 *Celsr3*$^{-/-}$ embryos; $P < 0.0001$, wild type versus mutant, Mann-Whitney test). To further investigate the requirement of Celsr3 in the response to ephrinA reverse signaling, we used a Dunn chamber growth cone turning assay[12,33]. Motor neurons were dissected from lumbar LMC and cultured on laminin-coated coverslips to allow initial axonal growth. Coverslips were then inverted in Dunn chambers in which GDNF and EphA7-Fc were added to the outer well to generate a gradient across the bridge (inner-well-low to outer-well-high gradient) (**Fig. 5**). We measured the initial angle (α)

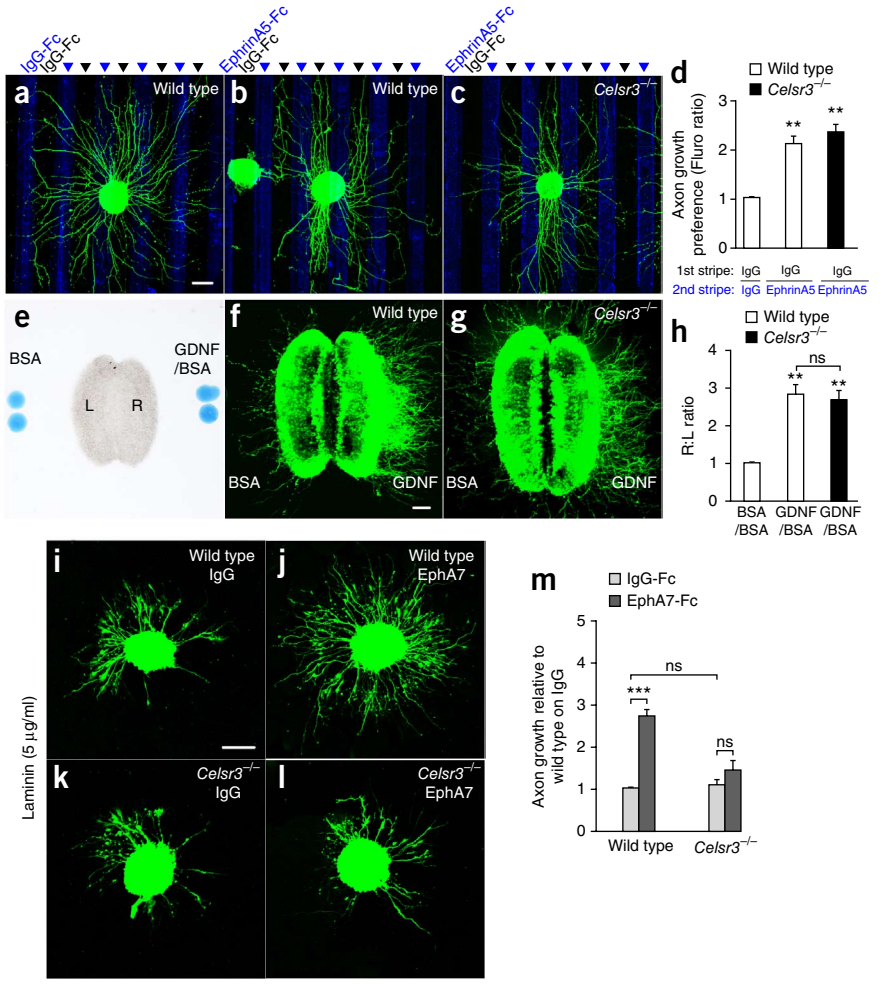

Figure 4 Celsr3-deficient LMC axons respond to GDNF and forward signaling but not to reverse signaling. (**a**–**c**) Stripe assay with LMC explants (*Hb9::GFP*-positive). (**a**) wild type LMC motor axons on IgG-Fc/IgG-Fc stripes. (**b**) wild type LMC motor axons on IgG-Fc/ephrinA5-Fc alternating stripes. (**c**) Celsr3-deficient LMC motor axons on IgG-Fc/ephrinA5-Fc alternating stripes. (**d**) Ratio of LMC motor axon growth on the first and second stripes ($n = 4$, 6 and 8 for first, second and third columns; $^{**}P < 0.01$, $P = 0.0022$ for wild type and $P = 0.0011$ for *Celsr3*$^{-/-}$, unpaired *t*-test versus wild type on IgG/IgG). Wild type and *Celsr3* mutant axons were similarly repelled by ephrinA5. (**e**–**g**) Bead attraction assay (**e**). Illustration of bead placement lateral to the E12.5 lumbar spinal cord explant. Wild type (**f**) and *Celsr3*$^{-/-}$ mutant (**g**) motor axons grew preferentially toward GDNF. (**h**) Relative right to left ratio of motor axons outgrowth when subjected to BSA from both sides (BSA/BSA, $n = 6$ embryos), or to GDNF (right) and BSA (left). GDNF potentiated axonal growth equally in the wild type ($n = 10$) and *Celsr3* mutants ($n = 12$ embryos); $^{**}P = 0.0043$ for wild type and 0.0044 for *Celsr3*$^{-/-}$; ns, not significant: $P = 0.5887$; Mann-Whitney test. (**i**–**l**) Axon outgrowth on IgG-Fc (**i**,**k**) and EphA7-Fc (**j**,**l**) of LMC explants isolated from wild type (**i**,**j**) and *Celsr3* mutants (**k**,**l**). (**m**) Quantification of axon growth from wild type and *Celsr3* mutant LMC explants relative to wild type on IgG-Fc. $n = 73$ explants on IgG and 70 on EphA7 from 6 wild type embryos, $n = 42$ explants on IgG and 39 on EphA7 from 3 *Celsr3*$^{-/-}$ embryos, $^{***}P < 0.0001$, wild type versus *Celsr3*$^{-/-}$ on IgG-Fc; ns, $P = 0.6568$, *Celsr3*$^{-/-}$ on IgG-Fc versus *Celsr3*$^{-/-}$ on EphA7-Fc and $P = 0.1811$; Mann-Whitney test. Error bars in **d**,**h**,**m** are mean ± s.e.m. Scale bars, 100 µm (**a**,**f**,**i**). Scale bar in **a** applies to **b** and **c**, bar in **f** to **g**, and bar in **i** to **j**–**l**.

between the direction of the axon and that of the gradient and, after 2 h in culture, the turning angle (β) between the initial and final direction of the axon. Turning angles are considered positive when axons grow toward the outer well and negative when they grow toward the inner well. As previously reported[12], GNDF or EphA7-Fc alone had no effect on directional growth, but their combination produced a significant attraction of wild type motor axons (**Fig. 5b**–**g**). In contrast, this attraction was completely lost for LMC neurons isolated from *Celsr3*$^{-/-}$ embryos (**Fig 5c**,**h** and **Supplementary Fig. 6a**,**b**,**e**). Importantly, mutant axons were still attracted by hepatocyte growth factor, a known positive cue in turning assay[33] (**Supplementary Fig. 6c**–**e**), demonstrating that Celsr3 is required in the growth cones to perceive the attractive effect of ephrinA reverse signaling.

Interactions between Celsr3 and ephrinA reverse signaling

Mutations in *Epha4* or *Celsr3* result in abnormalities of the peroneal nerve, and Celsr3 is necessary in the growth cones to elicit the attractive effect of ephrinA reverse signaling. To test potential interactions between *Epha4* and *Celsr3*, we crossed *Epha4*$^{+/-}$;*Celsr3*$^{+/-}$ double heterozygotes and analyzed the peroneal nerve projections of the progeny. The severity of the phenotype varies between the different *Epha4* mutant alleles[13]. In our crosses, *Epha4*$^{-/-}$ embryos had thinner but not truncated peroneal nerves (**Fig. 6a**,**c**,**e**). We did not observe any defects in *Celsr3*$^{+/-}$;*Epha4*$^{+/-}$ (**Fig. 6b**,**e**) or *Celsr2*$^{+/-}$;*Celsr3*$^{+/-}$;*Epha4*$^{+/-}$ (**Supplementary Fig. 7a**,**b**,**e**) mice. By contrast, the Celsr3 phenotype was exacerbated when one or both copies of Epha4 were mutated (mean thickness of the deep peroneal nerve ± s.e.m.: 47.6 ± 1.38 µm in wild type ($n = 12$), 47.4 ± 0.83 µm in *Celsr2*$^{+/-}$;*Celsr3*$^{+/-}$;*Epha4*$^{+/-}$ ($n = 14$), 31.6 ± 0.81 µm in *Epha4*$^{-/-}$ ($n = 22$), 16.5 µm ± 1.65 in *Celsr3*$^{-/-}$ ($n = 20$), 12.8 µm ± 0.97 in *Celsr3*$^{-/-}$;*Epha4*$^{+/-}$ ($n = 18$) and 10.2 ± 0.88 µm in *Celsr3*$^{-/-}$;*Epha4*$^{-/-}$ ($n = 12$); **Fig. 6c**–**e** and **Supplementary Fig. 7a**–**e**). These results suggest that *Celsr3* and *Epha4* cooperatively control the pathfinding of motor axons that innervate the dorsal hindlimb.

In addition to their expression in the ventral limb, where they serve as ligands for EphA forward signaling, ephrinA2 and ephrinA5 are also expressed in LMC$_L$ axons, where they behave as receptors for EphAs expressed in dorsal mesenchyme. To investigate whether Celsr3 interacts physically with ephrinA2 or ephrinA5, we transfected HEK293T (human embryonic kidney) cells to express Celsr3-GFP alone, Celsr3-GFP plus Myc-ephrinA2, or Celsr3-GFP plus Myc-ephrinA5. We used anti-Myc antibodies for immunoprecipitation and anti-GFP for western blotting. When Celsr3 was transfected to express either ephrinA2 or ephrinA5, Celsr3-GFP was detected in immunoprecipitates (**Fig. 6f**). By contrast, no Celsr3-GFP signal was seen in absence of ephrinAs (**Fig. 6f**). This indicates that Celsr3 is able to interact physically with ephrinA2 and ephrinA5 *in vitro*, an interaction that may underlie the functional cooperation *in vivo*.

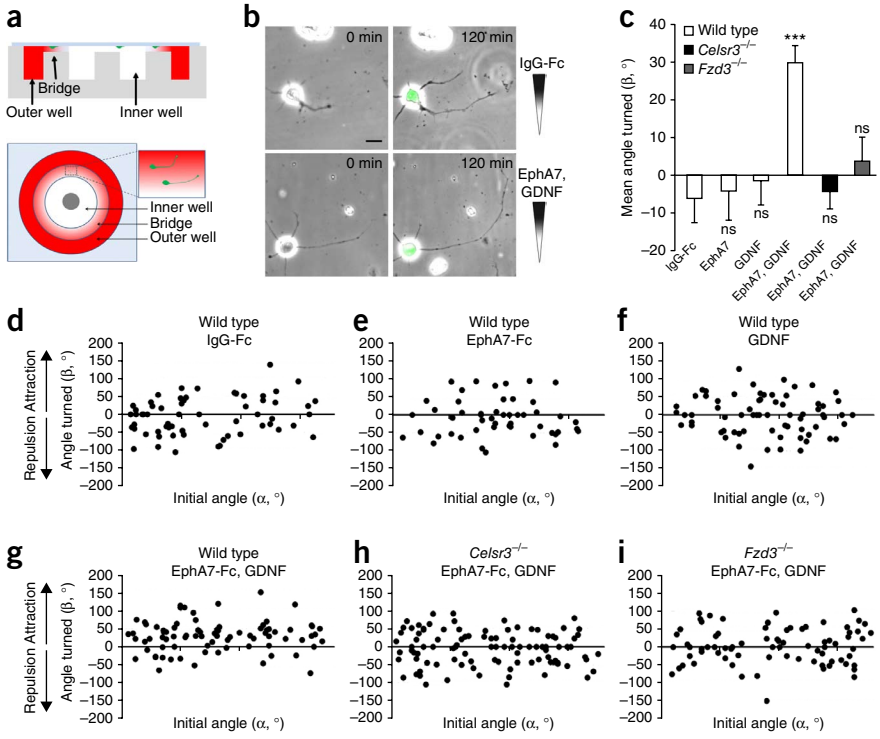

Figure 5 Celsr3 is required for attraction of LMC axons by EphA7 and GDNF in the axon turning assay. (**a**) Lateral and top views of the Dunn chamber. EphA7 and/or GDNF are added to the outer well to form a gradient across the bridge. (**b**) Examples of control LMC motor axons growth (labeled with *Hb9::GFP*) from the starting point (0 min) to the end of experiment (120 min). Axons turn toward the EphA7-Fc and GDNF source, but not toward IgG-Fc. (**c**) Angle turned β (mean ± s.e.m.) of wild type, *Celsr3*$^{-/-}$ and *Fzd3*$^{-/-}$ motor axons in different conditions. ns, $P > 0.05$; ***$P < 0.001$. $P = 0.8486$, wild type in EphA7-Fc gradient; $P = 0.6119$, wild type in GDNF gradient; $P < 0.0001$, wild type in EphA7-Fc plus GDNF gradient; $P = 0.8183$, *Celsr3*$^{-/-}$ in EphA7-Fc+GDNF gradient; $P = 0.3077$, *Fzd3*$^{-/-}$ in EphA7-Fc plus GDNF gradient; unpaired *t*-test versus Wild type in IgG-Fc gradient. (**d**–**i**) Scatter plots of turned angles β versus initial angles α ($5° < \alpha < 175°$) in the indicated conditions. Wild type motor axons: IgG-Fc, $n = 63$; EphA7-Fc, $n = 52$; GDNF, $n = 69$; EphA7-Fc plus GDNF, $n = 83$. *Celsr3*$^{-/-}$ motor axons: EphA7-Fc plus GDNF, $n = 100$. *Fzd3*$^{-/-}$ motor axons: EphA7-Fc plus GDNF, $n = 60$. 3 independent experiments were performed for each condition. Scale bar, 10 µm.

LMC$_L$ axons are defective in *Fzd3* but not in *Vangl2* mutants

In the developing nervous system, Fzd3 and Celsr3 are essential for axon guidance[18,21]. *Fzd3*$^{-/-}$ and *Celsr3*$^{-/-}$ mice have common defects in major axonal tracts such as the anterior commissure, internal capsule, medial lemniscus and corticospinal tract[14,19]. Furthermore, *Celsr3*$^{-/-}$, *Fzd3*$^{-/-}$ and *Vangl2*$^{Lp/Lp}$ mutant mice exhibit errors in axon projections of monoaminergic neurons in the brainstem and commissural interneurons in the spinal cord[16,22,34]. We studied *Fzd3* and *Vangl2* expression and found that it overlapped that of Celsr3 in the lumbar spinal cord (**Fig. 7a–d**). We generated new *Fzd3* alleles using the knockout first (ko) construct from EUCOMM (http://www.sanger.ac.uk/mouseportal/search?query=fzd3) (**Supplementary Fig. 8a–c**). RT-PCR amplification and sequencing showed that three different mRNA isoforms were produced in *Fzd3*$^{ko/ko}$ mice (**Supplementary Fig. 8a**). In the first isoform, the engrailed-2 (*En2*) splice acceptor is ignored, leading to the production of a wild type transcript. In the second, the *En2 lacZ* fusion cassette, inserted in intron 2, is transcribed as anticipated. In the third, a cryptic splice donor in the *En2* exon results in the inclusion of a 115-nucleotide exon in the wild type mRNA downstream of exon2 (**Supplementary Fig. 8d**), leading to a reading frame shift. We analyzed projections of motor axons in *Fzd3*$^{-/-}$ and *Vangl2*$^{-/-}$ embryos, as well as the limb morphology and locomotor behavior in *Fzd3*$^{ko/ko}$, *Fzd3*$^{fl/-}$;*Isl1::Cre* and *Vangl2*$^{fl/-}$;*Isl1::Cre* mice. *Vangl2* null mutants were derived from the floxed allele[35]. In contrast to *Fzd3*$^{-/-}$ animals, which die at birth[19], a small proportion of *Fzd3*$^{ko/ko}$ mice survived for a few weeks, showing

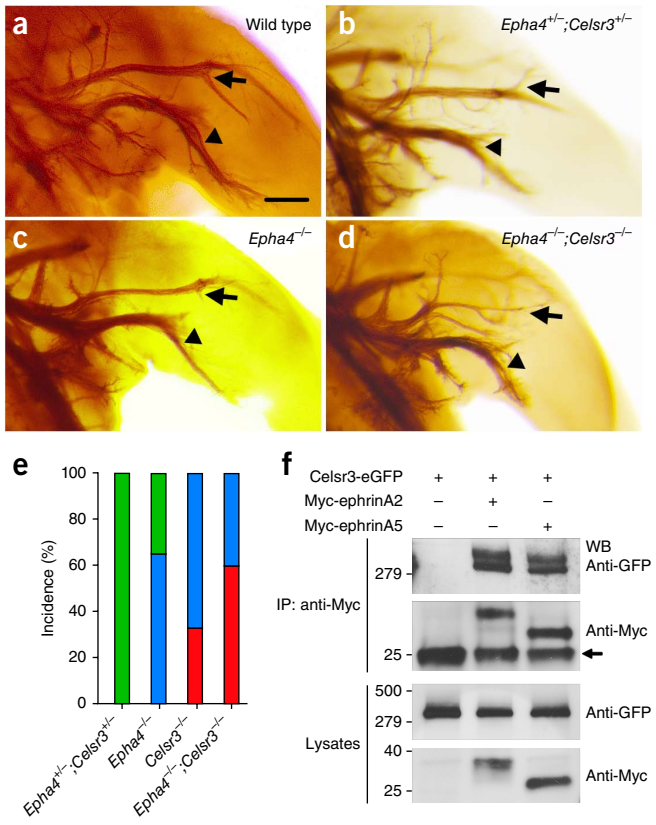

Figure 6 Interactions between Celsr3 and EphA-ephrinA signaling. (**a**–**d**) Lateral views of sciatic nerves stained by anti–neurofilament 160 in wild type (**a**), *Epha4*$^{+/-}$;*Celsr3*$^{+/-}$ (**b**), *Epha4*$^{-/-}$ (**c**) and *Epha4*$^{-/-}$;*Celsr3*$^{-/-}$ (**d**) embryos at E12.5. Arrows, peroneal nerve; arrowheads, tibial nerve. (**e**) Incidence of different phenotypes in wild type and mutant mice: green, normal; blue, thinning; red, severe reduction. *Epha4*$^{+/-}$;*Celsr3*$^{+/-}$, $n = 20$; *Epha4*$^{-/-}$, $n = 30$; *Celsr3*$^{-/-}$, $n = 52$; *Epha4*$^{-/-}$;*Celsr3*$^{-/-}$, $n = 10$. (**f**) Coimmunoprecipitation (IP) of Myc-ephrinA2 or Myc-ephrinA5 and Celsr3-eGFP in transfected HEK293T cells. Upon IP with anti-Myc, western blotting (WB) showed an interaction between Celsr3-eGFP and Myc-ephrinA2 or Myc-ephrinA5. Arrow, IgG light chain. Full-length blots are shown in **Supplementary Figure 11**. Scale bar, 200 µm.

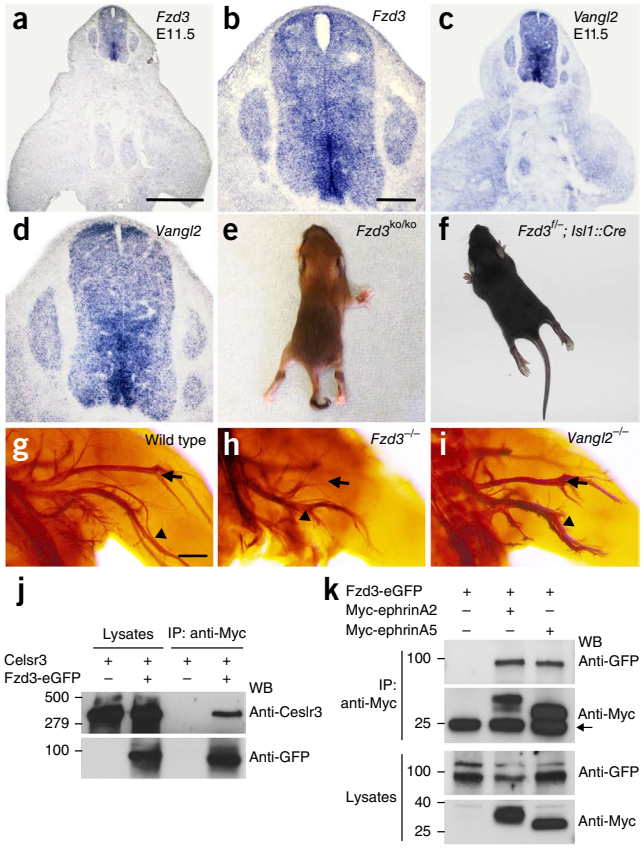

Figure 7 Peroneal nerve projections are *Fzd3* dependent and *Vangl2* independent. (**a**–**d**) Transverse sections of E11.5 embryos at the level of the lumbar spinal cord and hindlimbs, hybridized with digoxigenin-labeled *Fzd3* (**a**,**b**) or *Vangl2* (**c**,**d**) probes. The experiment was performed twice. (**e**) $Fzd3^{ko/ko}$ mouse with stiff hindlimbs and looptail phenotype. (**f**) $Fzd3^{fl-}$;*Isl1::Cre* mouse with stiff hindlimbs. (**g**–**i**) Lateral views of sciatic nerve revealed by anti–neurofilament 160 staining at E12.5, in wild type (**g**, $n = 32$), $Fzd3^{-/-}$ (**h**, $n = 48$) and $Vangl2^{-/-}$ (**i**, $n = 12$) embryos. Arrows, peroneal nerve; arrowheads, tibial nerve. (**j**,**k**) Coimmunoprecipitation (IP) assays between Celsr3 and Fzd3-eGFP (**j**) and Myc-ephrinA2 or Myc-ephrinA5 and Fzd3-eGFP (**k**) in transfected HEK293T cells. Fzd3-eGFP interacted with Celsr3, Myc-ephrinA2 and Myc-ephrinA5. Arrow, IgG light chain; WB, western blot. Full-length blots are shown in **Supplementary Figure 11**. Scale bars: 500 µm (**a**,**c**); 100 µm (**b**,**d**); 200 µm (**g**–**i**).

that the ko allele behaves as a hypomorphic allele. Surviving $Fzd3^{ko/ko}$ mice had a looping tail and paralyzed hindlimbs (**Fig. 7e** and **Supplementary Movie 3**), suggesting that Fzd3 is important for hindlimb innervation.

To investigate this further, we removed the *lacZ-neo* cassette and used the resulting conditional allele, in which exon 3 is flanked by *loxP* sites ($Fzd3^{f}$), to generate $Fzd3^{-/-}$ and $Fzd3^{fl-}$;*Isl1::Cre* mice (**Supplementary Fig. 8b**,**c**). Neurofilament staining of whole-mount $Fzd3^{-/-}$ embryos showed that the peroneal nerve was truncated in all embryos examined (**Fig. 7g**,**h**; $n = 48$). *Fzd3*-deficient axons failed to respond to the combination of GNDF and EphA7-Fc in the growth cone turning assay (**Fig. 5c**,**i**) and to EphA7-Fc in the axon outgrowth assay (fold induction of axon outgrowth by EphA7-Fc versus IgG-Fc: 2.73 in wild type and 1.13 in $Fzd3^{-/-}$; $n = 73$ explants on IgG and 70 on EphA7 from 6 wild type embryos, $n = 37$ explants on IgG and 35 on EphA7 from 3 $Fzd3^{-/-}$ embryos; $P < 0.0001$, wild type versus mutant, Mann-Whitney test). $Fzd3^{fl-}$;*Isl1::Cre* mice exhibited hindlimb deformities and reduced deep peroneal nerves (**Fig. 7f** and **Supplementary Fig. 8e**,**h**,**j**). In sharp contrast to *Celsr3* and *Fzd3* mutant mice, $Vangl2^{fl-}$;*Isl1::Cre* mice did not display any motor deficit or hindlimb malformation, and $Vangl2^{-/-}$ *embryos* did not show any abnormality in the peroneal nerve (**Fig. 7g**,**i**; deep peroneal mean width 39.9 µm in wild type and 40.1 µm in $Vangl2^{-/-}$, $n = 12$). We analyzed $Celsr3^{+/-}$;$Fzd3^{+/-}$ and $Celsr2^{+/-}$;$Celsr3^{+/-}$;$Fzd3^{+/-}$ heterozygous embryos and did not observe any reduction in the deep peroneal nerve at E12.5 ($n = 16$ and 10 embryos for $Celsr3^{+/-}$;$Fzd3^{+/-}$ and $Celsr2^{+/-}$;$Celsr3^{+/-}$;$Fzd3^{+/-}$; **Supplementary Fig. 8e**–**j**).

In HEK293T cells, Fzd3 immunoprecipitated with Celsr3 (**Fig. 7j**), ephrinA2 and ephrinA5 (**Fig. 7k**). However, we did not detect interactions between Vangl2 and ephrinA2 or A5 (**Supplementary Fig. 9a**). Given the synergistic function of EphA-ephrinA reverse signaling and GDNF-GFRα1 signaling integrated by Ret[12], we tested the physical interactions between Celsr3, Fzd3, Ret and GFRα1. We found that both Celsr3 and Fzd3 coimmunoprecipitated with Ret and GFRα1 in transfected cells (**Supplementary Fig. 9b**,**c**). In contrast, we did not detect positive interactions between Celsr3/Fzd3 and EphA7 (**Supplementary Fig. 9d**,**e**). Taken together, these results suggest the existence, in the growth cones of lumbar motor neurons, of a complex that contains ephrinAs, Ret, GFRα1, Celsr3 and Fzd3.

DISCUSSION

Inactivation of Celsr3 in motor neurons impaired the extension of LMC_L axons into the dorsal hindlimb and led to defective innervation of dorsal muscles, congenital clubfoot and stiffness of the limb. *Celsr3* is expressed in motor neurons but not in the limb mesenchyme. Therefore, Celsr3-mediated homophilic interactions between growth cones of LMC_L neurons and mesenchymal cells are unlikely. The expressivity of the *Celsr3* phenotype was enhanced when *Celsr2* was similarly mutated, and a similar high expressivity was observed in *Fzd3* mutants. These results provide evidence that Celsr3 and Fzd3 cooperatively regulate axon guidance in the PNS, as they do in CNS[14,19] and enteric nervous system[36]. The LMC_L axon projection and hindlimb phenotypes were not seen in $Vangl2^{-/-}$ mice, suggesting that Vangl2 is dispensable for guidance of motor axon. This was unexpected because, like *Celsr3* and *Fzd3*, *Vangl2* is a core PCP gene, implicated in guidance of spinal commissural and hindbrain monoaminergic axons in the brainstem[16,22]. A possible explanation may be the dominant negative activity or the gain of function associated with the looptail (*Lp*) mutation used in the latter studies. The $Vangl2^{Lp}$ allele encodes a mutated protein that may interfere with the function of the endogenous Vangl2 and/or with other components of PCP signaling[37].

Like *Celsr3* mutants, *Epha4*-deficient mice have locomotor defects and abnormal development of the corticospinal tract and anterior commissure[38]. In addition, the different *Epha4* mutant alleles have variable penetrance of the hindlimb phenotype[6,13]. Paralysis of muscles of the anterior compartment is caused by ventral rerouting of *Epha4* mutant LMC_L axons, which follow LMC_M axons into an enlarged tibial nerve. The ventral extension of mutant LMC_L motor axons, which normally express high levels of EphA4 (refs. 6,7,39,40), is attributed to their incapability to respond to a repulsive signal from the ventral limb triggered by ephrinAs[6]. A similar thin peroneal nerve with aberrant ventral rerouting of LMC_L axons is also seen in mice with defective GDNF-Ret-GFRα1 signaling[13,33]. Notably, the *Celsr3* phenotype was reminiscent of, yet different from, the *Epha4* or *Ret* phenotype: *Celsr3* mutant axons stalled at the branching point of the peroneal nerve, but never grew ventrally. Consistent with this, *Celsr3* mutant axons were repelled by ephrinA2 and ephrinA5 in stripe

assays, exactly like their wild type counterparts. Despite phenotypic differences, the defective peroneal nerves in *Celsr3*, *Fzd3*, *Epha4* and *Ret* mutants, and the increased penetrance of the peroneal nerve phenotype in *Celsr3*$^{-/-}$;*Epha4*$^{+/-}$ and *Celsr3*$^{-/-}$;*Epha4*$^{-/-}$ (this study) or *Epha4*$^{-/-}$;*Ret*$^{-/-}$ (ref. 13) double mutants, suggest that some underlying mechanisms may be shared.

Analysis of *Epha4* mice, on the one hand, and *Ret* or *Gdnf* mice, on the other hand, led to the conclusion that, in addition to EphA4 forward signaling that repels LMC_L from the ventral limb, other cues attract them dorsally. These axons are sensitive to branching and attractive signals from dorsal mesenchyme mediated by GDNF and ephrinA reverse signaling[4,10–13,33]. Ret in motor axon growth cones is believed to integrate signals generated by secreted GDNF and EphA on the surface of dorsal limb mesenchymal cells, thereby acting as a coincidence detector[12]. The segregation of ephrinA and EphA in distinct membrane microdomains allows the coexistence of forward and reverse ephrin-Eph signaling in the same growth cone[10]. There are five ephrinA and nine EphA genes, and many are expressed in motor neurons and mesenchymal cells. Therefore, functional redundancy hampers a direct genetic testing of the relative importance of different EphAs and ephrinAs, and of the respective contributions of EphA forward and ephrinA reverse signaling to the hindlimb innervation. Nevertheless, an important finding is that, in axon outgrowth and turning assays, *Celsr3* and *Fzd3* mutant axons, unlike wild type axons[11,12], were indifferent to ephrinA reverse signaling (**Supplementary Fig. 10a**,**b**). The fact that Celsr3, Fzd3 and Ret immunoprecipitate with ephrinAs suggests that these components form a signaling complex (**Supplementary Fig. 10c**). A key function of Celsr proteins and Fzd3 could be to organize, together with ephrinAs, membrane microdomains and thereby enable axon growth cones to resolve multiple, sometimes opposing signals.

In humans, clubfoot is a frequent developmental disorder affecting more than 1 in 1,000 live births. Its incidence varies with the ethnic group[41–43]. Family history and the higher concordance for clubfoot in monozygotic than dizygotic twins provide evidence for a genetic contribution to the pathology. Clubfoot can be idiopathic (when limb deformity occurs in isolation) or syndromic (associated with other malformations). Syndromic clubfoot is often associated with neurological and neuromuscular disorders, such as abnormal nerve conduction and spina bifida[44]. While *PITX1* and *TBR4*, two transcription factor genes whose mouse orthologs are expressed exclusively in the hindlimb, may be associated with idiopathic clubfoot[43], no genes have been clearly implicated in syndromic forms as yet. Our results suggest that *CELSR3* and *FZD3* may be candidates. Hypomorphic mutations, such as the *Fzd3*^{ko} allele described here in mice, are compatible with life and may lead to subtle neurological abnormalities and clubfoot.

METHODS

Methods and any associated references are available in the online version of the paper.

Note: Any Supplementary Information and Source Data files are available in the online version of the paper.

ACKNOWLEDGMENTS

We thank D. Bonanomi for advice on culture of explants; Y.-C. Lai for help with muscle dissection; J. Nathans for discussions; I. Dudanova (Max Planck Institute of Neurobiology), S. Evans (University of California, San Diego), T. Jessell (Columbia University), R. Klein (Max Planck Institute of Neurobiology), P. Vanderhaeghen (Université Libre de Bruxelles) and Y. Yang (US National Institutes of Health) for providing mutant mice; and John Flanagan (Harvard Medical School) for gift of the Myc-ephrinA2 and A5 plasmids. This work was supported by the following grants: Actions de Recherches Concertées (ARC-10/15-026), FRSM 3.4550.11, FNRS T0002.13, Interuniversity Poles of Attraction (SSTC, PAI p6/20 and PAI7/20), Fondation médicale Reine Elisabeth, Fondation JED-Belgique, and WELBIO-CR-2012A-07 from the Région Wallonne, all from Belgium. G.C., F.C. and F.T. are, respectively, research fellow, research associate and senior research associate from the Belgian Fund for Scientific Research (FNRS).

AUTHOR CONTRIBUTIONS

G.C. performed experiments, analyzed the data and wrote the manuscript; L.Z. characterized the locomotor behavior of Celsr3 mutant mice, M.M. conducted the electrophysiology study; F.H. and F.C. contributed analytical tools and commented on the manuscript, A.M.G. conducted the data analyses; F.T. supervised the project, analyzed the data and wrote the manuscript.

COMPETING FINANCIAL INTERESTS

The authors declare no competing financial interests.

1. Kolodkin, A.L. & Tessier-Lavigne, M. Mechanisms and molecules of neuronal wiring: a primer. *Cold Spring Harb. Perspect. Biol.* **3**, a001727 (2011).
2. Jessell, T.M., Surmeli, G. & Kelly, J.S. Motor neurons and the sense of place. *Neuron* **72**, 419–424 (2011).
3. Francius, C. & Clotman, F. Generating spinal motor neuron diversity: a long quest for neuronal identity. *Cell. Mol. Life Sci.* **71**, 813–829 (2014).
4. Bonanomi, D. & Pfaff, S.L. Motor axon pathfinding. *Cold Spring Harb. Perspect. Biol.* **2**, a001735 (2010).
5. Dudanova, I. & Klein, R. Integration of guidance cues: parallel signaling and crosstalk. *Trends Neurosci.* **36**, 295–304 (2013).
6. Helmbacher, F., Schneider-Maunoury, S., Topilko, P., Tiret, L. & Charnay, P. Targeting of the EphA4 tyrosine kinase receptor affects dorsal/ventral pathfinding of limb motor axons. *Development* **127**, 3313–3324 (2000).
7. Kania, A. & Jessell, T.M. Topographic motor projections in the limb imposed by LIM homeodomain protein regulation of ephrin-A:EphA interactions. *Neuron* **38**, 581–596 (2003).
8. Eberhart, J., Swartz, M.E., Koblar, S.A., Pasquale, E.B. & Krull, C.E. EphA4 constitutes a population-specific guidance cue for motor neurons. *Dev. Biol.* **247**, 89–101 (2002).
9. Kao, T.J., Law, C. & Kania, A. Eph and ephrin signaling: lessons learned from spinal motor neurons. *Semin. Cell Dev. Biol.* **23**, 83–91 (2012).
10. Marquardt, T. *et al.* Coexpressed EphA receptors and ephrin-A ligands mediate opposing actions on growth cone navigation from distinct membrane domains. *Cell* **121**, 127–139 (2005).
11. Dudanova, I. *et al.* Genetic evidence for a contribution of EphA-ephrinA reverse signaling to motor axon guidance. *J. Neurosci.* **32**, 5209–5215 (2012).
12. Bonanomi, D. *et al.* Ret is a multifunctional coreceptor that integrates diffusible- and contact-axon guidance signals. *Cell* **148**, 568–582 (2012).
13. Kramer, E.R. *et al.* Cooperation between GDNF/Ret and ephrinA/EphA4 signals for motor-axon pathway selection in the limb. *Neuron* **50**, 35–47 (2006).
14. Tissir, F., Bar, I., Jossin, Y., De Backer, O. & Goffinet, A.M. Protocadherin Celsr3 is crucial in axonal tract development. *Nat. Neurosci.* **8**, 451–457 (2005).
15. Zhou, L. *et al.* Early forebrain wiring: genetic dissection using conditional Celsr3 mutant mice. *Science* **320**, 946–949 (2008).
16. Fenstermaker, A.G. *et al.* Wnt/planar cell polarity signaling controls the anterior-posterior organization of monoaminergic axons in the brainstem. *J. Neurosci.* **30**, 16053–16064 (2010).
17. Price, D.J. *et al.* The development of cortical connections. *Eur. J. Neurosci.* **23**, 910–920 (2006).
18. Wang, Y. & Nathans, J. Tissue/planar cell polarity in vertebrates: new insights and new questions. *Development* **134**, 647–658 (2007).
19. Wang, Y., Thekdi, N., Smallwood, P.M., Macke, J.P. & Nathans, J. Frizzled-3 is required for the development of major fiber tracts in the rostral CNS. *J. Neurosci.* **22**, 8563–8573 (2002).
20. Wang, Y., Zhang, J., Mori, S. & Nathans, J. Axonal growth and guidance defects in Frizzled3 knock-out mice: a comparison of diffusion tensor magnetic resonance imaging, neurofilament staining, and genetically directed cell labeling. *J. Neurosci.* **26**, 355–364 (2006).
21. Hua, Z.L., Smallwood, P.M. & Nathans, J. Frizzled3 controls axonal development in distinct populations of cranial and spinal motor neurons. *Elife* **2**, e01482 (2013).
22. Shafer, B., Onishi, K., Lo, C., Colakoglu, G. & Zou, Y. Vangl2 promotes Wnt/planar cell polarity-like signaling by antagonizing Dvl1-mediated feedback inhibition in growth cone guidance. *Dev. Cell* **20**, 177–191 (2011).
23. Yang, L. *et al.* Isl1Cre reveals a common Bmp pathway in heart and limb development. *Development* **133**, 1575–1585 (2006).
24. Dessaud, E. *et al.* Interpretation of the sonic hedgehog morphogen gradient by a temporal adaptation mechanism. *Nature* **450**, 717–720 (2007).
25. Danielian, P.S., Muccino, D., Rowitch, D.H., Michael, S.K. & McMahon, A.P. Modification of gene activity in mouse embryos in utero by a tamoxifen-inducible form of Cre recombinase. *Curr. Biol.* **8**, 1323–1326 (1998).

26. Wang, L., Klein, R., Zheng, B. & Marquardt, T. Anatomical coupling of sensory and motor nerve trajectory via axon tracking. *Neuron* **71**, 263–277 (2011).
27. Sytkowski, A.J., Vogel, Z. & Nirenberg, M.W. Development of acetylcholine receptor clusters on cultured muscle cells. *Proc. Natl. Acad. Sci. USA* **70**, 270–274 (1973).
28. Gomez, C.M. *et al.* Slow-channel transgenic mice: a model of postsynaptic organellar degeneration at the neuromuscular junction. *J. Neurosci.* **17**, 4170–4179 (1997).
29. Tissir, F., De-Backer, O., Goffinet, A.M. & Lambert de Rouvroit, C. Developmental expression profiles of Celsr (Flamingo) genes in the mouse. *Mech. Dev.* **112**, 157–160 (2002).
30. Tissir, F. & Goffinet, A.M. Planar cell polarity signaling in neural development. *Curr. Opin. Neurobiol.* **20**, 572–577 (2010).
31. Kania, A., Johnson, R.L. & Jessell, T.M. Coordinate roles for LIM homeobox genes in directing the dorsoventral trajectory of motor axons in the vertebrate limb. *Cell* **102**, 161–173 (2000).
32. Haase, G. *et al.* GDNF acts through PEA3 to regulate cell body positioning and muscle innervation of specific motor neuron pools. *Neuron* **35**, 893–905 (2002).
33. Dudanova, I., Gatto, G. & Klein, R. GDNF acts as a chemoattractant to support ephrinA-induced repulsion of limb motor axons. *Curr. Biol.* **20**, 2150–2156 (2010).
34. Lyuksyutova, A.I. *et al.* Anterior-posterior guidance of commissural axons by Wnt-frizzled signaling. *Science* **302**, 1984–1988 (2003).
35. Song, H. *et al.* Planar cell polarity breaks bilateral symmetry by controlling ciliary positioning. *Nature* **466**, 378–382 (2010).
36. Sasselli, V. *et al.* Planar cell polarity genes control the connectivity of enteric neurons. *J. Clin. Invest.* **123**, 1763–1772 (2013).
37. Yin, H., Copley, C.O., Goodrich, L.V. & Deans, M.R. Comparison of phenotypes between different vangl2 mutants demonstrates dominant effects of the Looptail mutation during hair cell development. *PLoS ONE* **7**, e31988 (2012).
38. Kullander, K. *et al.* Role of EphA4 and EphrinB3 in local neuronal circuits that control walking. *Science* **299**, 1889–1892 (2003).
39. Eberhart, J. *et al.* Expression of EphA4, ephrin-A2 and ephrin-A5 during axon outgrowth to the hindlimb indicates potential roles in pathfinding. *Dev. Neurosci.* **22**, 237–250 (2000).
40. Iwamasa, H. *et al.* Expression of Eph receptor tyrosine kinases and their ligands in chick embryonic motor neurons and hindlimb muscles. *Dev. Growth Differ.* **41**, 685–698 (1999).
41. Carey, M., Bower, C., Mylvaganam, A. & Rouse, I. Talipes equinovarus in Western Australia. *Paediatr. Perinat. Epidemiol.* **17**, 187–194 (2003).
42. Chapman, C., Stott, N.S., Port, R.V. & Nicol, R.O. Genetics of club foot in Maori and Pacific people. *J. Med. Genet.* **37**, 680–683 (2000).
43. Dobbs, M.B. & Gurnett, C.A. Genetics of clubfoot. *J. Pediatr. Orthop. B* **21**, 7–9 (2012).
44. Nadeem, R.D., Brown, J.K., Lawson, G. & Macnicol, M.F. Somatosensory evoked potentials as a means of assessing neurological abnormality in congenital talipes equinovarus. *Dev. Med. Child Neurol.* **42**, 525–530 (2000).

ONLINE METHODS

Mutant mice. All animal procedures were carried out in accordance with European guidelines and approved by the animal ethics committee of the Université catholique de Louvain. *Celsr2*, *Celsr3*, *Isl1::Cre*, *Wnt1::Cre*, *Olig2::Cre*, *Vangl2*, and *Epha4* mutant mice were described previously[14,15,23,24,35,38,45]. *Hb9::GFP* mice were purchased from Jackson Laboratory. *Fzd3* mutants were generated as described in **Supplementary Figure 8**.

***In situ* hybridization.** Plasmids containing cDNA fragments of *Celsr2*, *Celsr3*, *Fzd3* or *Vangl2* were labeled using digoxigenin, as described previously[46]. Cryostat sections at the level of the lumbar spinal cord and hindlimbs were prepared from E11.5 and E12.5 embryos. They were treated with 1 µg/ml proteinase K in 0.1 M Tris-HCl, pH 8 and 10 mM EDTA, rinsed in DEPC-treated water and acetylated for 10 min at room temperature in 0.25 M acetic anhydride, 0.1 M triethanolamine. Slides were incubated overnight at 65 °C in a humidified chamber with denatured probes (1 µg/ml) in hybridization solution (50% formamide, 10% dextran sulfate, 0.3 M NaCl, 20 mM Tris-HCl, pH 7.5, 5 mM EDTA, 1× Denhardt's solution, 0.6 mg/ml yeast tRNA and 0.1% SDS). Slides were washed for 30 min at 65 °C in 50% formamide, 2× SSC, rinsed in 2× SSC, and treated for 1 h at 37 °C with 1 µg/ml RNase A in NTE buffer (0.5 M NaCl, 10 mM Tris-HCl pH 7.5, 5 mM EDTA). Slides were washed in 2× SSC and 0.2× SSC at 65 °C for 1 h each, blocked with 20% sheep serum and incubated overnight with alkaline phosphatase–coupled digoxigenin antibodies (1/2,000; Roche, 11093274910). Illustrations were prepared and edited with Adobe Photoshop.

Retrograde tracing. E12.5 or E13.5 embryos were eviscerated and cultured in DMEM/F-12 (Invitrogen), gassed with 95% O_2/5% CO_2 at 30 °C. Tetramethylrhodamine-conjugated lysine fixable dextran (3,000 MW, 50%, Invitrogen, D3308) was injected in the stump of the ventral tibial nerve, visualized with *Hb9::GFP*, after severing with microscissors. Embryos were cultured for ~6 h at 30 °C, fixed in 4% PFA and then cryosectioned for immunostaining.

Stripe assay. Stripes of ephrin-A5-Fc (R&D Systems, 374-EA) or IgG-Fc (R&D Systems, 110-HG) were printed on coverslips as reported in ref. 47. The coverslips were first coated with poly-D-lysine (PDL, 1 mg/ml, Sigma) and then with proteins (10 µg/ml) clustered by Cy3-conjugated anti–human Fc antibody or nonconjugated antibody (2:1, Jackson ImmunoResearch, 109-165-098 and 109-005-098), using a stripe-coating silicone matrix (M. Bastmeyer, Karlsruher Institute of Technology, Germany). Coverslips were coated with laminin (100 µg/ml, Invitrogen, 23017-015). LMC motor explants were dissected as described[48]. They were cultured on printed coverslips in MN medium (Neurobasal medium with B27, 2 mM Glutamax, 25 µM L-glutamic acid, 100 units/ml penicillin and 100 µg/ml streptomycin, Invitrogen), for 20 h, with 10 ng/ml GDNF (R&D Systems, 512-GF).

Dunn chamber assay. Dunn chamber assays were performed as described[33]. Briefly, LMC motor neurons were dissected and dissociated with 0.025% trypsin in L15 medium. Motor neurons were seeded on coverslips coated with PDL and laminin (50 µg/ml) and cultured in MN medium for 4 to 5 h. The Dunn chamber (Hawksley & Sons Ltd., UK) was assembled as fast as possible. Control MN medium in the outer well was exchanged for MN medium containing hepatocyte growth factor (50 ng/ml, 2207-HG), GDNF (200 ng/ml) or EphA7-Fc (5 µg/ml, 608-A7) clustered by anti-human Fc antibody (5:1), or GDNF and EphA7-Fc together. Images were captured at culture time zero and once again after 2 h in culture, using an inverted fluorescence phase contrast microscope (Zeiss).

Neurite outgrowth assay. 30 µg/ml EphA7-Fc or 10 µg/ml IgG-Fc (R&D Systems) was preclustered by 6 µg/ml anti-human Fc antibodies for 1 h at room temperature, and then mixed with 5 µg/ml laminin. PDL precoated coverslips (BD Biosciences, 354086) were coated for 3–5 h at 37 °C before use. E12.5 LMC motor explants were dissected, transferred to the coated coverslips, and cultured in MN medium at 37 °C for ~15 h.

Bead attraction assay. The bead attraction assay was performed as described[12]. Lumbar spinal cord was dissected and flattened in an open-book preparation from E12.5 Hb9::GFP-positive embryos. The caudal half was embedded in a rat tail collagen (50 µl):Matrigel (30 µl) mix (BD Biosciences) after removing the lateral, nonfluorescent part (keeping the left and right motor columns and the floor plate). Affi-Gel blue agarose beads (Bio-Rad) soaked with 1 µg/ml GDNF or BSA (4 °C overnight) were placed lateral to the explants in the gel. The explants were cultured in MN medium at 37 °C for ~15–20 h.

Culture of spinal motor neurons. LMC motor neurons were dissociated from E12.5 embryos as in the Dunn chamber assay. Motor neurons were divided equally into two wells and cultured in MN medium on laminin (50 µg/ml) precoated coverslips at 37 °C. To estimate the initial number of motor neurons, cells of the first well were fixed in 2% PFA, 15% sucrose after 5 h and the number of *Hb9::GFP* positive neurons counted. Cells of the second well were counted after 3 d in culture and the two numbers were used to calculate the percentage survival.

LMC motor neuron count. Wild type and *Celsr3*$^{-/-}$ embryos at E11.5, E12.5 and E13.5 were cryosectioned at 14 µm thickness from caudal to rostral lumbar spinal cord. Sections were collected once every five sections and immunostained with Foxp1 and Isl1. The numbers of motor neurons were counted manually with the help of NIH ImageJ software.

Quantification of axon outgrowth. Axon outgrowth of LMC explants were quantified with the FeatureJ plugin of ImageJ software. Images were first converted into 8-bit format and then processed with FeatureJ Hessian which can detect the linear axons automatically. After removing the outline of the explants manually, the total axon area was measured in pixels.

DNA constructs. For Celsr3-eGFP, eGFP was cloned from pEGFP-N1 (GenBank U55762) and inserted in-frame at position 8866 in the mouse *Celsr3* ORF in pcDNA3 (Invitrogen). This resulted in the production of a Celsr3 protein in which the 346 C-terminal amino acids are deleted and replaced by eGFP. For Fzd3-eGFP, the mouse *Fzd3* coding sequence (in pcDNA-Fzd3) was subcloned in pEGFP-N1 in-frame and 5′ to *eGFP*. Vangl2-DsRed was produced by cloning the full mouse *Vangl2* ORF in pDsRed-N1 (Clontech) in-frame and 5′ to the DsRed sequence. Myc-ephrinA2 and Myc-ephrinA5 were generously provided by J. Flanagan[49] (Harvard Medical School). Myc-GFRα1 and Myc-Ret were purchased from OriGene and EphA7-Myc from Sino Biological.

Immunostaining and antibodies. Embryos were fixed in 4% paraformaldehyde (PFA), cryoprotected in sucrose and then cryosectioned for immunostaining. Primary antibodies and reagents were goat anti-Foxp1 (1:1,000, R&D, AF4534), goat anti-neuropilin1 (1:100, R&D, AF566), mouse anti–neurofilament 160 (1:400, Sigma, N5264), rabbit anti-EphA4 (1:500, Santa Cruz, sc-921), rabbit anti-Ret (1:100, Santa Cruz, sc-167), rabbit anti–cleaved caspase3 (1:500, Cell Signaling, 9661), chick anti-GFP (1:1,000, Aves, GFP-1020), rabbit anti-GFP (1:2,000, Invitrogen, A11122), Alexa 594–conjugated α-bungarotoxin (1:2,000, Invitrogen, B-13423) and mouse anti-Islet1 (1:400, 3F7 from DSHB).

Whole-mount neurofilament staining. Embryos were dissected in PBS and fixed overnight in cold Dent's solution (one part DMSO, four parts methanol). After bleaching in one part 30% H_2O_2, two parts Dent's solution overnight at room temperature and washing in TBS three times, the embryos were incubated overnight at room temperature in blocking serum (1 part DMSO, 4 parts normal goat serum) containing mouse monoclonal anti–neurofilament 160 antibody (1:400, Sigma, N5264). Embryos were washed in TBSGT (TBS, 1% Triton-X100, 0.2% fish gelatin) eight times, 1 h each, at room temperature. They were incubated overnight at room temperature in blocking serum with peroxidase-conjugated anti–mouse IgG (Fab specific) (1:500, Sigma, A3682 or Jackson ImmunoResearch, 115-036-072). Embryos were washed in TBSGT eight times and then stained in DAB solution (0.05% DAB, 0.02% H_2O_2 in TBS) for 5 to 30 min. After staining, samples were dehydrated in 50% and 100% methanol and cleared in BABB solution (one part benzyl alcohol, two parts benzyl benzoate). Images were captured using a stereomicroscope (Leica) and edited using Adobe Photoshop.

Coimmunoprecipitation and western blotting. For coimmunoprecipitation assays, HEK293T cells were seeded into six-well plates and transfected with plasmids using Lipofectamine 2000 (Invitrogen). After 24 h culture, cells were lysed

doi:10.1038/nn.3784

for 2 h at 4 °C in lysis buffer containing 10 mM Tris-HCl (pH7.4), 137 mM NaCl, 2 mM EDTA, 10% glycerol, 0.5% Triton X-100,1% β-octylglucoside (Thermo Scientific), protease inhibitor cocktail (Roche Applied Science, 11836170001) and phosphatase inhibitor cocktail (Thermo Scientific, 1862495). Cell lysates were then centrifuged at 13,000*g* for 15 min at 4 °C. 40 µl supernatant was mixed with 10 µl 5× SDS-loading buffer and heated at 95 °C for 2 min or 50 °C for 30 min (for Celsr3-eGFP) as total lysates. The remaining supernatant was incubated with 2 µg of mouse anti-Myc antibody (Santa Cruz, sc-40) overnight at 4 °C, followed by incubation with protein A/G beads (Santa Cruz) for 2 h at 4 °C. The beads were washed four times with lysis buffer and suspended in 40 µl 2× SDS-loading buffer. Total lysates and immunoprecipitates were further separated by SDS-PAGE and analyzed by immunoblotting. Primary antibodies we used were mouse anti-Myc (1:1,000, Santa Cruz, sc-40), rabbit anti-Myc (1:1,500, Santa Cruz, sc-789), rabbit anti-GFP (1:2,000, Chemicon/Millipore, AB3080), rabbit anti-DsRed (1:1,000, Clontech, 632496) and mouse anti-Celsr3 (1:1,000, 11E3)[15].

Statistics. No statistical methods were used to predetermine sample sizes, but our sample sizes are similar to those reported in previous publications[12,13]. Randomization and blinding were not employed. Data were tested for normality using the Shapiro-Wilk test, and compared by using either Student's *t*-test, for normally distributed data, or the Mann-Whitney *U*-test for non-normally distributed ones. Analyses were carried out using GraphPad Prism.

A Supplementary Methods checklist is available.

45. Tissir, F. *et al.* Lack of cadherins Celsr2 and Celsr3 impairs ependymal ciliogenesis, leading to fatal hydrocephalus. *Nat. Neurosci.* **13**, 700–707 (2010).
46. Zhou, L. *et al.* Maturation of "neocortex isole" *in vivo* in mice. *J. Neurosci.* **30**, 7928–7939 (2010).
47. Knöll, B., Weinl, C., Nordheim, A. & Bonhoeffer, F. Stripe assay to examine axonal guidance and cell migration. *Nat. Protoc.* **2**, 1216–1224 (2007).
48. Wang, L. & Marquardt, T. Direct live monitoring of heterotypic axon-axon interactions *in vitro*. *Nat. Protoc.* **7**, 351–363 (2012).
49. Feldheim, D.A. *et al.* Topographic guidance labels in a sensory projection to the forebrain. *Neuron* **21**, 1303–1313 (1998).

Supplemental data:

The supplemental data includes 2 supplemental figures and 2 movies

Figure S1 and Movie S1 are related to Figure 1

Figure S2 and Movie S2 are related to Figure 7

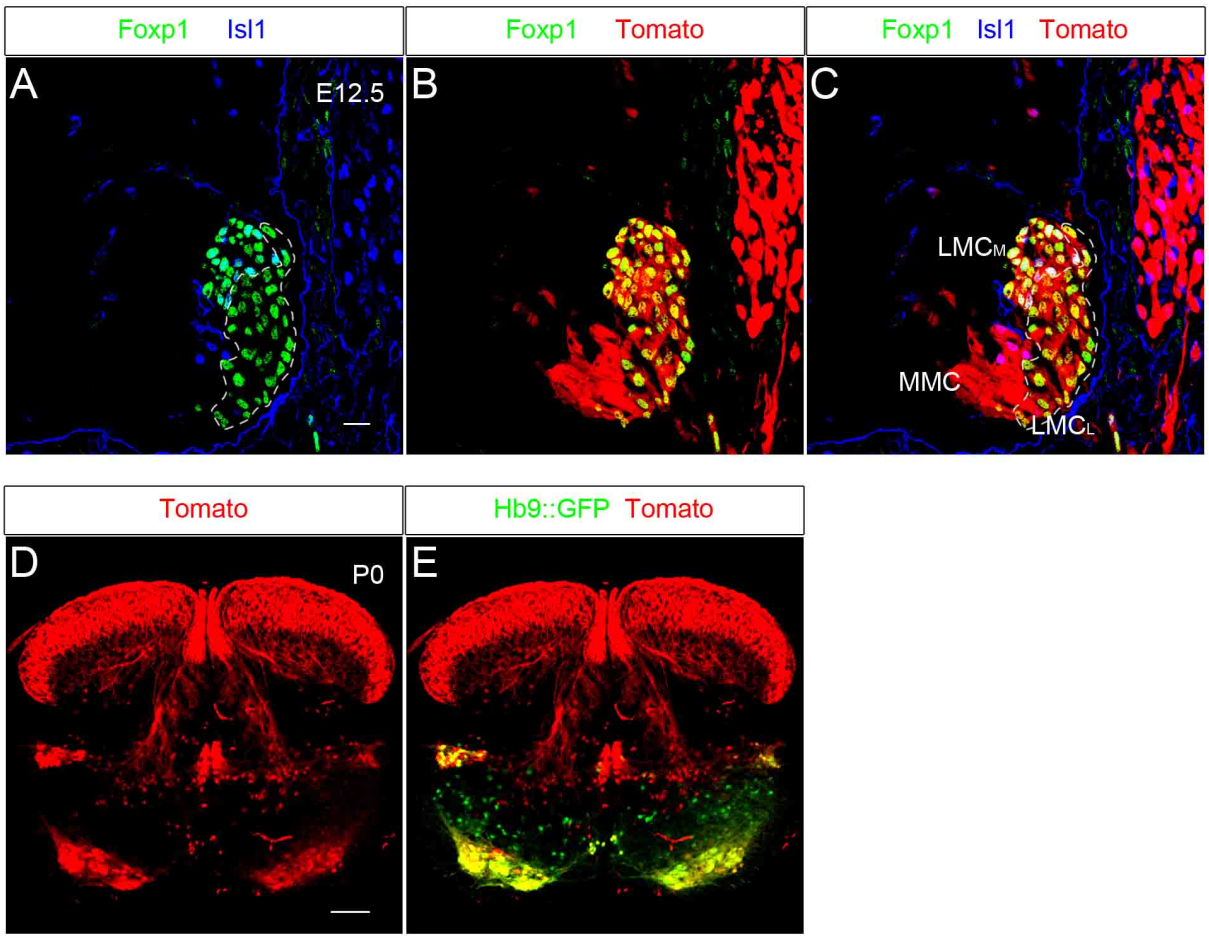

Figure S1: Lineage Labeling of *Isl1::Cre*–positive Cells and their Descendants (related to Figure 1)

(A–C) Cross sections of lumbar spinal cord of *Rosa26–Tomato* ; *Isl1::Cre* embryos at E12.5. *Isl1::Cre* (red) is expressed in all spinal motor neurons and DRG neurons. Foxp1 (green) and Isl1 (blue) antibodies were used to highlight LMC_M and LMC_L.

(D and E) Cross sections of lumbar spinal cord of *Rosa26–Tomato* ; *Isl1::Cre* newborns (P0). *Isl1::Cre* (red) is expressed in motor neurons in the ventral horn of the spinal cord, co–labeled by the transgene *Hb9::GFP* in (E); in sensory neurons in the dorsal horn, as well as in projections of DRG neurons.

Scale bar: 10 µm in A–C; 100 µm in D and E.

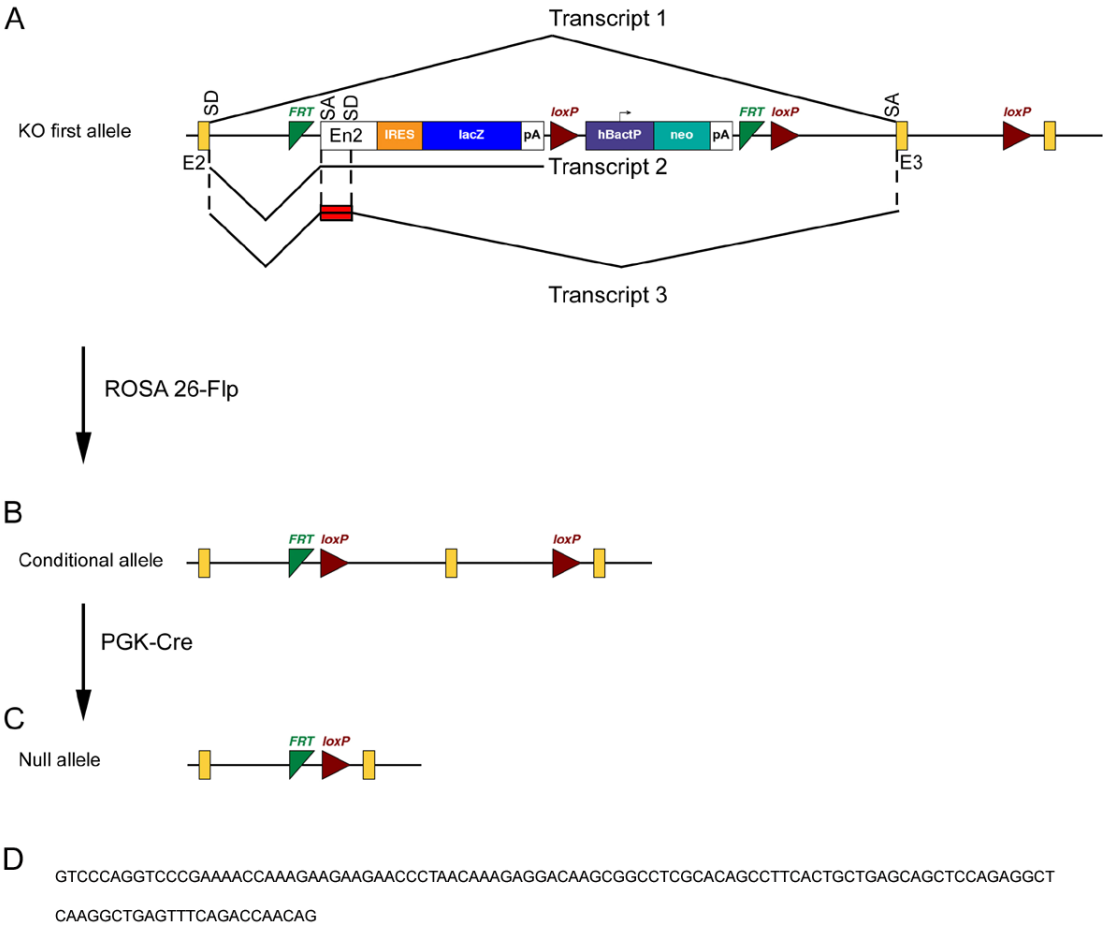

Figure S2: Generation of *Fzd3* mutant mice (related to Figure 7).

(A) Schematic representation of the knockout first allele (modified from EUCOMM). A cassette containing FTR-Engrailed–2 exon–IRES–LacZ–loxP–neo–FRT–loxP was inserted in intron 2. In $Fzd3^{ko/ko}$ mice, three mRNAs isoforms are produced. In the first, the engrailed2 splice acceptor is "ignored" leading to the production of the wild–type transcript. In the second, the engrailed–2–LacZ fusion cassette is transcribed as expected. In the third, a cryptic splice donor in the engrailed–2 exon results in a premature and aberrant splicing of the engrailed–2–LacZ cassette with the insertion of 115 nucleotides between exons 2 and 3 of the wild–type mRNA (red box).

(B) The conditional allele is obtained by removal of the FTR–Engrailed–2 –IREs–LacZ–loxP–neo–FRT cassette upon crossing with ROSA26–Flp. Exon 3 is flanked by two loxP sites thereby allowing its conditional excision.

(C) In the null allele, exon 3 was deleted in the germline by crossing the conditional allele with PGK::Cre.

(D) Nucleotide sequence of the Engrailed–2 “mini” exon found in transcript 3.

E2 and E3: exons 2 and 3 of the *Fzd3* gene. En2: Engrailed–2 exon, pA: polyadenylation site SA: splice acceptor, SD: splice donor.